Bottom-Up Synthesis of Necklace-Like Graphene Nanoribbons

Matthias Georg Schwab,[a] Akimitsu Narita,[a] Silvio Osella,[b] Yunbin Hu,[a] Ali Maghsoumi,[c] Alexey Mavrinsky,[a] Wojciech Pisula,[a, d] Chiara Castiglioni,[c] Matteo Tommasini,[c] David Beljonne,[b] Xinliang Feng,*[e] and Klaus Müllen*[a]

Manuscript received: April 30, 2015
Accepted Article published: June 9, 2015
Final Article published: July 2, 2015

[a] *Dr. M. G. Schwab,[+] Dr. A. Narita, Dr. Y. Hu, Dr. A. Mavrinsky, Prof. Dr. W. Pisula, Prof. Dr. K. Müllen*
Max Planck Institute for Polymer Research
Ackermannweg 10, 55128 Mainz (Germany)
E-mail: muellen@mpip-mainz.mpg.de

[b] *Dr. S. Osella, Dr. D. Beljonne*
Chemistry of Novel Materials
University of Mons
Place du Parc 20, 7000 Mons (Belgium)

[c] *A. Maghsoumi, Prof. Dr. C. Castiglioni, Prof. Dr. M. Tommasini*
Dipartimento di Chimica, Materiali ed Ingegneria Chimica "G. Natta", Politecnico di Milano
Piazza Leonardo da Vinci 32, 20133 Milano (Italy)

[d] *Prof. Dr. W. Pisula*
Department of Molecular Physics, Faculty of Chemistry
Lodz University of Technology
Zeromskiego 116, 90-924 Lodz (Poland)

[e] *Prof. Dr. X. Feng*
Center for Advancing Electronics Dresden (cfaed)
& Department of Chemistry and Food Chemistry
Dresden University of Technology
Walther-Hempel-Bau Mommsenstrasse 4, 01062 Dresden (Germany)
E-mail: xinliang.feng@tu-dresden.de

[+] *Present address:*
BASF SE
Carl-Bosch-Straße 38, 67056 Ludwigshafen (Germany)

Graphene nanoribbons (GNRs) are ribbon-shaped segments of graphene, which are attracting an increasing attention for their promising electronic properties.[1] With non-zero bandgaps induced by the lateral quantum confinement, GNRs are promising for future nano- and opto-electronic applications, in stark contrast to zero-bandgap graphene itself.[2] Whereas GNRs fabricated by top-down methods such as lithographic patterning of graphene[3] and unzipping of carbon nanotubes[4] lack the structural precision and reproducibility, bottom-up chemical synthesis based on solution-mediated[5] or surface-assisted[6] cyclodehydrogenation has enabled reproducible fabrication of GNRs with chemically defined and uniform structures.[7] Especially, the solution synthesis allows bulk-scale preparation of the GNRs, which can be processed from a liquid phase for fabrication of nanoelectronic devices.[8]

The width and the edge configuration of the GNRs have a critical effect on their optoelectronic properties, such as bandgaps, as theoretically[9] and experimentally[5d,6c,7] demonstrated. However, studies on the structure–property relationships of the GNRs have been mostly limited to those with specific edge structures, such as armchair, zigzag, and their hybrids, namely chiral, leaving the effect of the edge configurations still underexplored. Here, we report the synthesis of GNR **1** with an unprecedented "necklace-like" structure,[10] which features an armchair-type edge configuration (Figure 1). We further demonstrate the synthesis of a polycyclic aromatic hydrocarbon (PAH) **C84**, bearing 84 sp^2 carbon atoms in the aromatic core, as a model compound.

The electronic structures of **C84** and necklace-like GNR **1** has been investigated at the DFT level, with the HSE functional[11] and 6-31G* Pople basis set.[12] **C84** is thus predicted to have the highest occupied molecular orbital (HOMO) at −4.58 eV and the lowest unoccupied molecular orbital (LUMO) at −2.41 eV with an energy gap of 2.17 eV. Periodic boundary conditions applied to assess GNR **1** yield a band structure with the top of the valence band and the bottom of the conducting band located at −4.38 and −2.98 eV, respectively (see the Supporting Information). The corresponding bandgap of 1.40 eV is relatively larger as compared to other GNRs of similar width.[9c] Importantly, there has hitherto been no report on a synthesis of GNRs exhibiting a bandgap of around 1.4 eV.[5–7]

Next, in order to investigate the feasibility of the fabrication of necklace-like GNR **1** through the oxidative cyclodehydrogenation of polyphenylene precursor **10**, the synthesis of model compound **C84** was carried out as displayed in Scheme 1. 4,4′-Dibromo-2,2′-diiodo-1,1′-biphenyl (**2**)[13] was subjected to Sonogashira coupling with trimethylsilyl (TMS) acetylene at room temperature to selectively yield TMS-protected diethynylbiphenyl **3**, which was subsequently deprotected with potassium

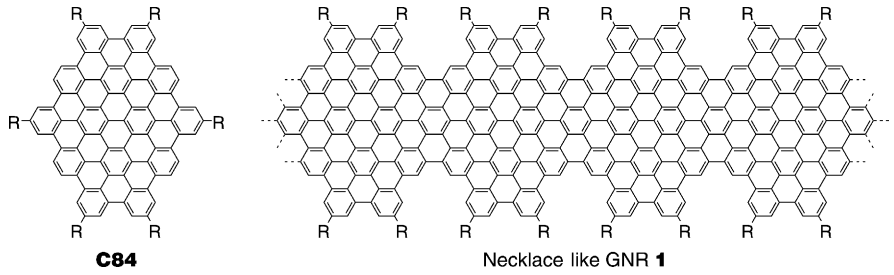

Figure 1. Structures of PAH **C84** and necklace-like GNR **1**. R: dodecyl.

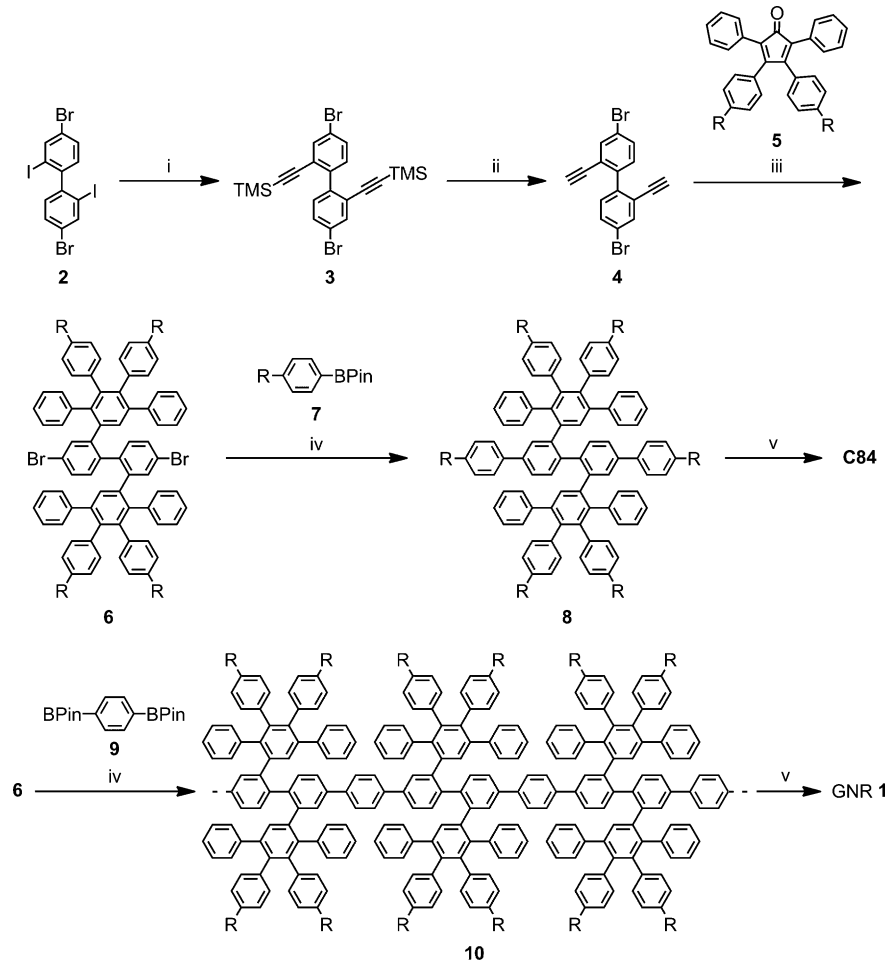

Scheme 1. Synthesis of **C84** and necklace-like GNR **1**. Reagents and conditions: (i) trimethylsilyl acetylene, $[Pd(PPh_3)_2Cl_2]$, CuI, NEt_3, rt, 62%; (ii) K_2CO_3, THF/MeOH, rt, 75%; (iii) *ortho*-xylene, 160 °C, μW, 300 W, 79%; (iv) $[Pd(PPh_3)_4]$, K_2CO_3, toluene, Aliquat 336, reflux: 76%; (v) $FeCl_3$, CH_2Cl_2/CH_3NO_2, rt, **C84**: 91%. R: dodecyl.

carbonate to form 4,4′-dibromo-2,2′-diethynyl-1,1′-biphenyl (**4**). Two-fold Diels–Alder cycloaddition of **4** with tetraphenylcyclopentadienone **5**[14] afforded oligophenylene **6**, which also serves as a monomer in the preparation of polyphenylene precursor **10** for necklace-like GNR **1** (Scheme 1).

Suzuki coupling of oligophenylene **6** with 4-dodecylphenylboronic acid pinacol ester (**7**) provided the corresponding oligophenylene precursor **8**. The cyclodehydrogenation of precursor **8** was successful with 7.5 equivalents of iron(III) chloride per hydrogen to be removed, providing **C84** in 91% isolated yield. Matrix-assisted laser desorption/ionization time-of-flight (MALDI-TOF) mass spectrometry (MS) analysis clearly demonstrated the elimination of 32 protons upon the cyclodehydrogenation and displayed the isotopic pattern of **C84** in perfect agreement with the simulation (Figure 2), proving the formation of **C84** without any partially fused species.[5a,15] Signals from chlorinated products were also observed, but such peaks could be overestimated.[15] ^{1}H NMR analysis of **C84** was attempted in 1,1,2,2-$[D_2]$tetrachloroethane, but peaks from aromatic protons could not be observed even at 140 °C, which was attributable to the strong aggregation in solution, similar to other large PAHs (Figure S4, Supporting Information).[5a,16] Nevertheless, the Fourier transform infrared (FTIR) spectrum of **C84** showed fingerprint peaks in agreement with DFT-based simulation, which provided further structural proof (Figure S16, Supporting Information). Among the great variety of PAHs thus far synthesized,[17] **C84** reported here is the first PAH with 84 sp^2 carbons in the aromatic core.

C84 with six dodecyl chains shows in the differential scanning calorimetry (DSC) scan one phase transition at 74 °C, which is related to the reorganization of alkyl side chains (Figure S5, Supporting Information), slightly affecting the supramolecular order. Two-dimensional wide-angle X-ray scattering (2D-WAXS) patterns of **C84** recorded at 30 and 90 °C indicate liquid crystallinity and the formation of columnar superstructures at both temperatures (Figure 3). Similar thermotropic properties have been observed for other core extended PAHs.[18] Equatorial small-angle reflections are assigned to a hexagonal unit cell of $a_{hex} = 3.25$ nm for the intercolumnar arrangement. In the stacks, the molecules are packed on top of each other due to π-stacking interactions with an intermolecular distance of 0.35 nm as derived from the wide-angle meridional reflections. The broad isotropic amorphous halo is attributed to side chains disordered in the columnar periphery, which is charac-

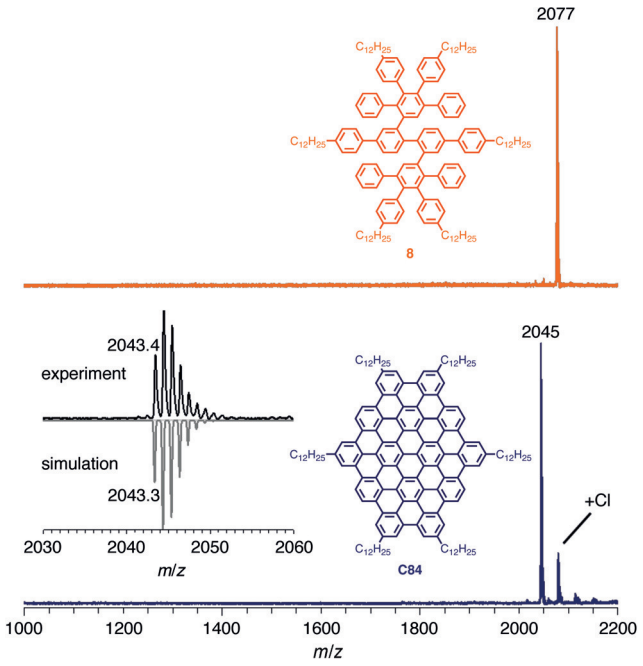

Figure 2. MALDI-TOF spectra of oligophenylene precursor **8** (top) and **C84** (bottom); the inset shows a comparison between the experimental (black) and simulated (gray) isotopic pattern of **C84**.

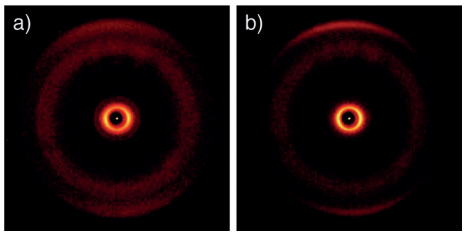

Figure 3. 2D-WAXS of **C84** at a) 30 °C and b) 90 °C.

teristic for a liquid crystalline phase. The LC organization remained unchanged for **C84** after cooling down the sample to 30 °C below the phase transition (Figure 3 a). However, broadening of the meridional reflections suggests a slightly decreased intracolumnar order. This minor change can be explained in terms of increased steric demand of the alkyl substituents.

Next, the synthesis of necklace-like GNR **1** was carried out starting from polyphenylene precursor **10** (Scheme 1). The repeating units of precursor **10** has the same arrangement of the aromatic rings as precursor **8**, which was demonstrated to undergo highly efficient cyclodehydrogenation, leading to the formation of **C84**. Hence, precursor **10** was prepared via a A_2B_2-type Suzuki polycondensation[8c,d,19] of oligophenylene monomer **6** and 1,4-benzenediboronic acid bis(pinacol) ester (**9**). To circumvent the stoichiometry problem of the A_2B_2-type polymerization[7,20] and achieve the highest possible polymerization efficiency, the monomers were thoroughly purified by using a recycling preparative size-exclusion chromatography (SEC) system before use and weighed with a great care (see the Supporting Information). After three days of refluxing, excess amounts of bromobenzene and then phenylboronic acid were added for the end-capping of the polymer. MALDI-TOF MS analysis of the resulting polymer precursor **10** showed a pattern of peaks, corresponding to the expected *m/z* values for **10**, extending over 17 000 (Figure S9, Supporting Information). Precursor **10** with molecular weight of about 17 000 has ten repeating units and is expected to yield GNR **1** with a length of approximately 13 nm.

SEC analysis of precursor **10** indicated its weight-average molecular weight (M_w) of 6900 g mol^{-1} and polydispersity index (PDI) of 1.7 against polystyrene (PS) standards. When poly(*p*-phenylene) (PPP) standards were applied M_w and PDI values were estimated to be 5100 g mol^{-1} and 1.5, respectively. Although these values based on the SEC analysis are only rough estimations according to the hydrodynamic volume of the solubilized polymer, they are useful for the comparison of different polyphenylene precursors of similar structures. The M_w of precursor **10** was smaller than that of a related polyphenylene prepared by AA-type Yamamoto polymerization,[5e] which is presumably because of the intrinsic stoichiometry problem of the A_2B_2-type Suzuki polymerization (see the Supporting Information)[7,20] as well as the higher steric demand in this system.[8e]

The cyclodehydrogenation of precursor **10** was performed using the condition optimized for precursor **8** to afford necklace-like GNR **1** (Scheme 1). MALDI-TOF MS analysis of GNR **1** revealed a pattern of broadened peaks for up to octamers with intervals approximately corresponding to the molecular weight of one repeating unit (Figure S9, Supporting Information). However, precise analysis was hindered by the limitation of the MALDI-TOF MS analysis for large aromatic molecules with broad molecular-weight distribution.[5e,8e,21]

Whereas elemental analysis is not reliable for such carbon-rich materials due to possible soot formation,[15] FTIR analysis provided more information about the efficiency of the cyclodehydrogenation (Figure 4 a). Precursor **10** reveals a peak at 4050 cm^{-1}, a non-fundamental IR absorption associated to the presence of free-rotating benzene rings, as well as a group of signals at 3026, 3053, and 3084 cm^{-1} characteristic for C–H stretching vibrations of aromatic rings.[5a,d,e,8e] These peaks are all starkly attenuated in the spectrum of GNR **1**. Moreover, out-of-plane (*opla*) C–H deformation bands at 699 and 764 cm^{-1} from mono-substituted benzene rings are strongly diminished and those at 815, 838, and 894 cm^{-1} from di-substituted benzene rings all disappeared after the cyclodehydrogenation.[5a,-d,e,8e] Considering the short length of GNR **1**, the remaining peaks at 693 and 758 cm^{-1} are probably from the phenyl groups introduced by the endcapping. Additionally, the peak at 719 cm^{-1} originates from the alkyl chains. Moreover, Raman spectrum of GNR **1** reveals characteristic D and G peaks as well as second-order peaks (Figure 4 b), which are typical of other structurally well-defined GNRs in the literature.[5a,b,d,e,6a] These observations underline the successful transformation of precursor **10** into GNR **1**.

Thanks to the long alkyl chains placed at the peripheral positions, GNR **1** could be dispersed in *N*-methylpyrrolidone (NMP) by mild sonication.[5a,e] The UV/Vis absorption spectrum of GNR

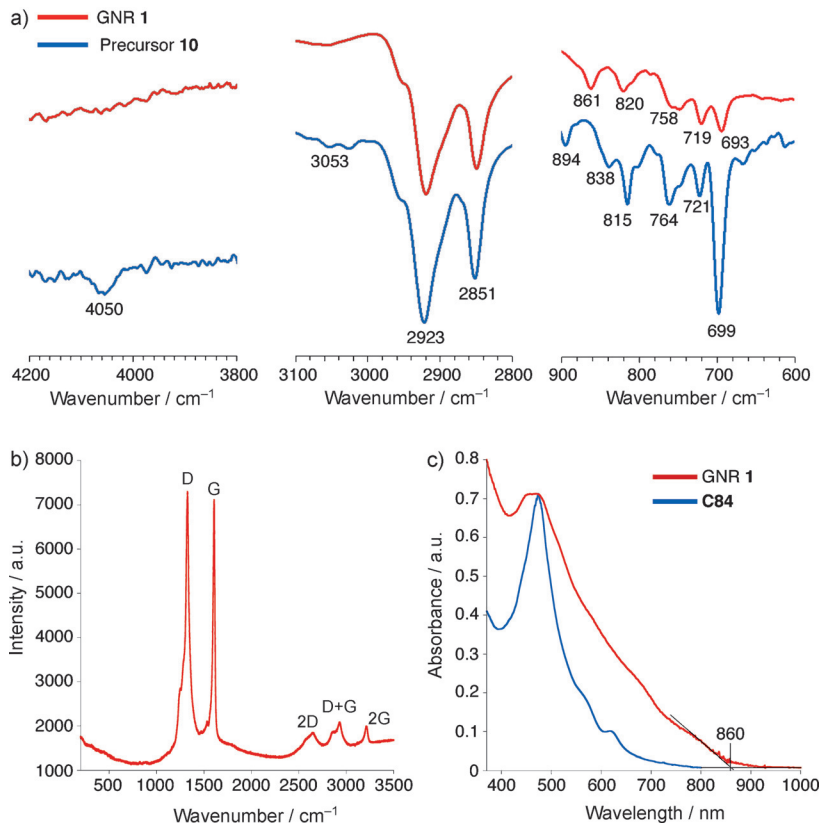

Figure 4. (a) Representative regions of the FTIR spectra of GNR **1** (red) and polyphenylene precursor **10** (blue). (b) Raman spectrum of GNR **1** at measured with excitation at 514.5 nm. (c) Normalized UV/Vis absorption spectra of **C84** in THF and GNR **1** in NMP.

1 was thus measured in NMP and compared with that of **C84** in tetrahydrofuran (THF) (Figures 4c, S6, and S12). **C84** was measured in THF because its solubility in NMP was limited. **C84** showed a prominent β-band at 473 nm with a molar extinction coefficient of 6864 $m^2 mol^{-1}$, with smaller peaks at 564 and 620 nm, corresponding to the *p*- and α-bands, respectively. The HOMO–LUMO gaps of PAHs are related to the *p*-bands, and this experimental observation is in good accordance with the theoretical gap of 2.17 eV (571 nm). On the other hand, GNR **1** displayed broadened peaks with an absorption maximum at around 465 nm and shoulders approximately at 510, 680, and 780 nm. The broadening of the spectrum is most likely caused by the presence of shorter GNRs, possessing different bandgaps that are dependent on the length.[5a,e,8e] Based on the absorption edge of 860 nm, the optical bandgap of longer GNRs contained in the obtained sample is estimated to be 1.44 eV, which again is well in line with the theoretically estimated bandgap of 1.40 eV. This result further validates the successful formation of GNR **1** and indicates that longer GNRs in the obtained sample are sufficiently elongated to possess the electronic band structure of the infinite GNR **1**.

In summary, we have synthesized an unprecedented PAH **C84** with 84 sp^2 carbons in the aromatic core and extended its synthesis to necklace-like GNR **1** applying A_2B_2-type Suzuki polymerization. Characterization by MALDI-TOF MS and FTIR, Raman, and UV/Vis absorption spectroscopy validated the successful formation of GNR **1** and demonstrated its optical bandgap of 1.44 eV in very good agreement with the theoretical value of 1.40 eV, which has not been attained with other GNR structures. Although the polymerization efficiency still needs to be improved to obtain longer necklace-like GNRs, this result contributes to the elucidation of structure–property relationships of GNRs and enables more precise tuning of their bandgap, which is of high importance for the future development of GNR-based nano- and opto-electronic devices.

Experimental Section

All the experimental and theoretical details are provided in the Supporting Information.

Acknowledgements

We are grateful for the financial support from the European Research Council grant on NANOGRAPH, DFG Priority Program SPP 1459, Graphene Flagship (No. CNECT-ICT-604391), and European Union Projects UPGRADE, GENIUS, and MoQuaS.

[1] X. Li, X. Wang, L. Zhang, S. Lee, H. Dai, *Science* **2008**, *319*, 1229–1232.
[2] a) J. Bai, Y. Huang, *Mater. Sci. Eng. R* **2010**, *70*, 341–353; b) K. S. Novoselov, V. I. Falko, L. Colombo, P. R. Gellert, M. G. Schwab, K. Kim, *Nature* **2012**, *490*, 192–200.
[3] a) Z. Chen, Y. Lin, M. Rooks, P. Avouris, *Physica E* **2007**, *40*, 228–232; b) M. Han, B. Özyilmaz, Y. Zhang, P. Kim, *Phys. Rev. Lett.* **2007**, *98*, 206805; c) A. N. Abbas, G. Liu, B. Liu, L. Zhang, H. Liu, D. Ohlberg, W. Wu, C. Zhou, *ACS Nano* **2014**, *8*, 1538–1546.
[4] a) D. V. Kosynkin, A. L. Higginbotham, A. Sinitskii, J. R. Lomeda, A. Dimiev, B. K. Price, J. M. Tour, *Nature* **2009**, *458*, 872–876; b) L. Jiao, L. Zhang, X. Wang, G. Diankov, H. Dai, *Nature* **2009**, *458*, 877–880.
[5] a) A. Narita, X. Feng, Y. Hernandez, S. A. Jensen, M. Bonn, H. Yang, I. A. Verzhbitskiy, C. Casiraghi, M. R. Hansen, A. H. R. Koch, G. Fytas, O. Ivasenko, B. Li, K. S. Mali, T. Balandina, S. Mahesh, S. De Feyter, K. Müllen, *Nat. Chem.* **2014**, *6*, 126–132; b) T. H. Vo, M. Shekhirev, D. A. Kunkel, M. D. Morton, E. Berglund, L. Kong, P. M. Wilson, P. A. Dowben, A. Enders, A. Sinitskii, *Nat. Commun.* **2014**, *5*, 3189; c) T. H. Vo, M. Shekhirev, D. A. Kunkel, F. Orange, M. J. F. Guinel, A. Enders, A. Sinitskii, *Chem. Commun.* **2014**, *50*, 4172–4174; d) A. Narita, I. A. Verzhbitskiy, W. Frederickx, K. S. Mali, S. A. Jensen, M. R. Hansen, M. Bonn, S. De Feyter, C. Casiraghi, X. Feng, K. Müllen, *ACS Nano* **2014**, *8*, 11622–11630; e) M. G. Schwab, A. Narita, Y. Hernandez, T. Balandina, K. S. Mali, S. De Feyter, X. Feng, K. Müllen, *J. Am. Chem. Soc.* **2012**, *134*, 18169–18172.

[6] a) J. Cai, P. Ruffieux, R. Jaafar, M. Bieri, T. Braun, S. Blankenburg, M. Muoth, A. P. Seitsonen, M. Saleh, X. Feng, K. Müllen, R. Fasel, *Nature* **2010**, *466*, 470 – 473; b) Y.-C. Chen, T. Cao, C. Chen, Z. Pedramrazi, D. Haberer, D. G. de Oteyza, F. R. Fischer, S. G. Louie, M. F. Crommie, *Nat. Nanotechnol.* **2015**, *10*, 156 – 160; c) H. Huang, D. Wei, J. Sun, S. L. Wong, Y. P. Feng, A. H. C. Neto, A. T. S. Wee, *Sci. Rep.* **2012**, *2*, 983.

[7] A. Narita, X. Feng, K. Müllen, *Chem. Rec.* **2015**, *15*, 295 – 309.

[8] a) A. N. Abbas, G. Liu, A. Narita, M. Orosco, X. Feng, K. Müllen, C. Zhou, *J. Am. Chem. Soc.* **2014**, *136*, 7555 – 7558; b) U. Zschieschang, H. Klauk, I. B. Müller, A. J. Strudwick, T. Hintermann, M. G. Schwab, A. Narita, X. Feng, K. Müllen, R. T. Weitz, *Adv. Electron Mater.* **2015**, *1*, 1400010; c) K. T. Kim, J. W. Lee, W. H. Jo, *Macromol. Chem. Phys.* **2013**, *214*, 2768 – 2773; d) K. T. Kim, J. W. Jung, W. H. Jo, *Carbon* **2013**, *63*, 202 – 209; e) M. El Gemayel, A. Narita, L. F. Dössel, R. S. Sundaram, A. Kiersnowski, W. Pisula, M. R. Hansen, A. C. Ferrari, E. Orgiu, X. Feng, K. Müllen, P. Samori, *Nanoscale* **2014**, *6*, 6301 – 6314.

[9] a) B. Obradovic, R. Kotlyar, F. Heinz, P. Matagne, T. Rakshit, M. D. Giles, M. A. Stettler, D. E. Nikonov, *Appl. Phys. Lett.* **2006**, *88*, 142102; b) J. Wang, R. Zhao, M. Yang, Z. Liu, *J. Chem. Phys.* **2013**, *138*, 084701; c) S. Osella, A. Narita, M. G. Schwab, Y. Hernandez, X. Feng, K. Müllen, D. Beljonne, *ACS Nano* **2012**, *6*, 5539 – 5548.

[10] X. Yan, Y. Cui, Q. He, K. Wang, J. Li, W. Mu, B. Wang, Z.-c. Ou-yang, *Chem. Eur. J.* **2008**, *14*, 5974 – 5980.

[11] J. Heyd, G. E. Scuseria, M. Ernzerhof, *J. Chem. Phys.* **2003**, *118*, 8207 – 8215.

[12] V. A. Rassolov, M. A. Ratner, J. A. Pople, P. C. Redfern, L. A. Curtiss, *J. Comput. Chem.* **2001**, *22*, 976 – 984.

[13] K. L. Chan, M. J. McKiernan, C. R. Towns, A. B. Holmes, *J. Am. Chem. Soc.* **2005**, *127*, 7662 – 7663.

[14] J. P. Hill, W. Jin, A. Kosaka, T. Fukushima, H. Ichihara, T. Shimomura, K. Ito, T. Hashizume, N. Ishii, T. Aida, *Science* **2004**, *304*, 1481 – 1483.

[15] C. D. Simpson, J. D. Brand, A. J. Berresheim, L. Przybilla, H. J. Räder, K. Müllen, *Chem. Eur. J.* **2002**, *8*, 1424 – 1429.

[16] a) D. Wasserfallen, M. Kastler, W. Pisula, W. A. Hofer, Y. Fogel, Z. Wang, K. Müllen, *J. Am. Chem. Soc.* **2006**, *128*, 1334 – 1339; b) M. Kastler, W. Pisula, D. Wasserfallen, T. Pakula, K. Müllen, *J. Am. Chem. Soc.* **2005**, *127*, 4286 – 4296.

[17] J. Wu, W. Pisula, K. Müllen, *Chem. Rev.* **2007**, *107*, 718 – 747.

[18] W. Pisula, ž. Tomović, C. Simpson, M. Kastler, T. Pakula, K. Müllen, *Chem. Mater.* **2005**, *17*, 4296 – 4303.

[19] L. Dössel, L. Gherghel, X. Feng, K. Müllen, *Angew. Chem. Int. Ed.* **2011**, *50*, 2540 – 2543; *Angew. Chem.* **2011**, *123*, 2588 – 2591.

[20] a) A. D. Schlüter, *J. Polym. Sci. Part A* **2001**, *39*, 1533 – 1556; b) W. H. Carothers, *Trans. Faraday Soc.* **1936**, *32*, 39 – 49.

[21] K. Martin, J. Spickermann, H. J. Räder, K. Müllen, *Rapid Commun. Mass Spectrom.* **1996**, *10*, 1471 – 1474.